

## Performance analysis of single and double passes flat plate collector with and without porous media

A. A. YOUSEF BASHRIA\*, N. MARIAH ADAM

This study involves a model to investigate the effect of mass flow, channel depth and collector length on the thermal performance and pressure drop through solar collectors by using a developed internet based mathematical modelling. The chosen development software tool is Dreamweaver combined with the Active Server Pages (ASP) as an extension environment and VBScript as scripting language. The developed program is capable of handling ambient conditions, collector characteristics, and material thermal properties. The criteria for solar systems in Malaysia were used as an input in the program to simulate the performance of the solar system. The solution procedure is performed for flat plate collector in single and double flow mode. It is concluded that the increase of the thermal efficiency is 10–12% for double flow when compared with single flow, and 8% after using porous media.

Key words: single and double flow solar air heater, porous media, thermal performance, pressure drop, flow channel depth

### Nomenclature

$A$	– area of collector that absorbs solar radiation [ $\text{m}^2$ ]	$h_{c,ga}$	– convective heat transfer coefficient between the glass and the ambient air [ $\text{W m}^{-2} \text{K}^{-1}$ ]
$A_f$	– fluid area [ $\text{m}^2$ ]	$I$	– solar radiation [ $\text{W m}^{-2}$ ]
$C_p$	– specific heat of working fluid [ $\text{J kg}^{-1} \text{K}^{-1}$ ]	$k$	– fluid thermal conductivity [ $\text{W m}^{-1} \text{K}^{-1}$ ]
$D$	– collector depth [m]	$L$	– collector length [m]
$D_h$	– hydraulic diameter [m]	$\dot{m}$	– collector flow rate [ $\text{kg sec}^{-1}$ ]
$f$	– friction factor	$N$	– number of glass cover
$F_R$	– heat removal factor	$Nu$	– Nusselt number
$h$	– fluid heat transfer coefficient [ $\text{W m}^{-2} \text{K}^{-1}$ ]	$P$	– pressure drop across the duct [Pa]
$h_r$	– radiation heat transfer coefficient [ $\text{W m}^{-2} \text{K}^{-1}$ ]	$Q_u$	– rate of useful energy gain [W]
		$Re$	– Reynolds number

Institute of Advanced Technology, Alternative and Renewable Energy Laboratories, University Putra Malaysia, 43400 UPM Serdang, Malaysia

\* Corresponding author, e-mail address: bashria@yahoo.com

$T_a$ – ambient air temperature [K]	$T_t$ – bottom plate temperature [K]
$T_c$ – cover temperature [K]	$U$ – overall heat loss coefficient [W m <sup>-2</sup> K <sup>-1</sup> ]
$T_f$ – fluid temperature [K]	$U_b$ – back loss coefficient [W m <sup>-2</sup> K <sup>-1</sup> ]
$T_i$ – fluid inlet temperature [K]	$U_t$ – top loss coefficient [W m <sup>-2</sup> K <sup>-1</sup> ]
$T_p$ – absorber plate surface temperature [K]	$V$ – wind velocity [m s <sup>-1</sup> ]
$T_{pr}$ – porous media temperature [K]	$W$ – collector width [m]

*Greek symbols*

$\varepsilon_p$ – emittance of absorber plate	$\tau$ – solar transmittance of glazing
$\varepsilon_c$ – emittance of glass cover	$\alpha$ – solar absorptance of collector plate
$\rho$ – air density [Kg m <sup>-3</sup> ]	$\mu$ – dynamic viscosity [Pa sec <sup>-1</sup> ]
$\sigma$ – Stephen-Boltzmann constant	

*Subscripts*

a – ambient	h – hydraulic
b – back	p – plate
c – cover	u – useful
f – fluid	

**1. Introduction**

Energy is a vital need in all aspects and due to the increasing demand for energy coupled with its inefficient consumption, the environment has been polluted either directly or indirectly. To prevent this from becoming a global disaster, it is inevitable to strengthen efforts of energy generation and utilization using sustainable means and progressively substituting the fossil fuels for renewable sources of energy. The solar radiation level in Malaysia is high, ranging from 6.6 kWh m<sup>-2</sup> in January to 6.0 kWh m<sup>-2</sup> in August, which is ideal for several solar energy applications [1].

Extensive investigations have been carried out on the optimum design of conventional and modified solar air heaters, in order to search for efficient and inexpensive designs suitable for mass production for different practical applications. The researchers have paid their attention to the effects of design and operational parameters, type of flow passes, number of glazing and type of absorber flat, corrugated or finned on the thermal performance of solar air heaters [2–5]. Ratna et al. [2] have presented theoretical parametric analysis of a corrugated solar air heater with and without cover, where they obtained the optimum flow channel depth, for maximum heat at lowest collector cost. Ratna et al. [3] have found that there exists an optimum mass flow rate corresponding to an optimum flow channel depth. This result has been concluded after conducting a study on 10 different designs of solar air heaters. Choudhury et al. [4] have calculated the ratio of the annual cost

and the annual energy gain for two-pass solar air heaters with single and double covers above the absorber. They concluded that for shorter duct lengths and lower air mass flow rates, the performance of the two pass air heaters with a single cover is most cost-effective as compared to the other designs. Karim and Hawlader [5] have performed an experimental study on three types of solar air collectors, i.e. flat plate, finned and corrugated absorbers. They reported that the V-corrugated is the most efficient collector and the flat plate collector is the least efficient. In spite of this concern on improving the performance of solar air heaters, little has been published on the effect of the air flow passage dimension on the efficiency and pressure drop and hence the cost-effectiveness of the system. Bashria et al. [6] and Bashria et al. [7] presented a developed internet based mathematical simulation to predict the thermal performance for different designs of solar air heaters.

The study presented in this article uses the aforementioned developed program to find the influence of different parameters, such as mass flow rate, flow channel depth and collector length on the system thermal performance and pressure drop through the collector, for flat plate collector in single and double passes, with and without using a porous media.

## 2. Theoretical analysis

Figure 1 shows schematically the cross sectional views and the thermal network of the solar air heaters investigated in the present work. In all types, the air heaters are composed of three plates, the cover, the absorber and the rear or back plate. The air flows in the upper channel depth between the cover and the absorber plate in Type-1 (i.e. single flow), but it is turned to continue flowing in the lower duct between the absorber and the rear plate in Type-2 and Type-3 (i.e. double flow). The lower duct has been packed with glass wool as a porous media of 0.80 porosity in Type-3. The various heat transfer coefficients at different components of the air heaters are illustrated in the thermal network in Fig. 1.

To model the three solar air collector types and obtain their relative equations, a number of simplifying assumptions are considered. These assumptions are as follows:

1. Performance is steady state
2. There is no absorption of solar energy by a cover insofar as it affects losses from the collector (i.e. the absorption of solar radiation in the cover is neglected)
3. Heat transfer fluid is considered a non-participating medium (i.e. the fluid is not participating in heat transfer)
4. The radiation coefficient between the two air duct surfaces is found by assuming a mean radiant temperature equal to the mean fluid temperature
5. Loss through front and back is to the same ambient temperature

Therefore the energy balance equations for the plates and the flowing air yield the following equations:

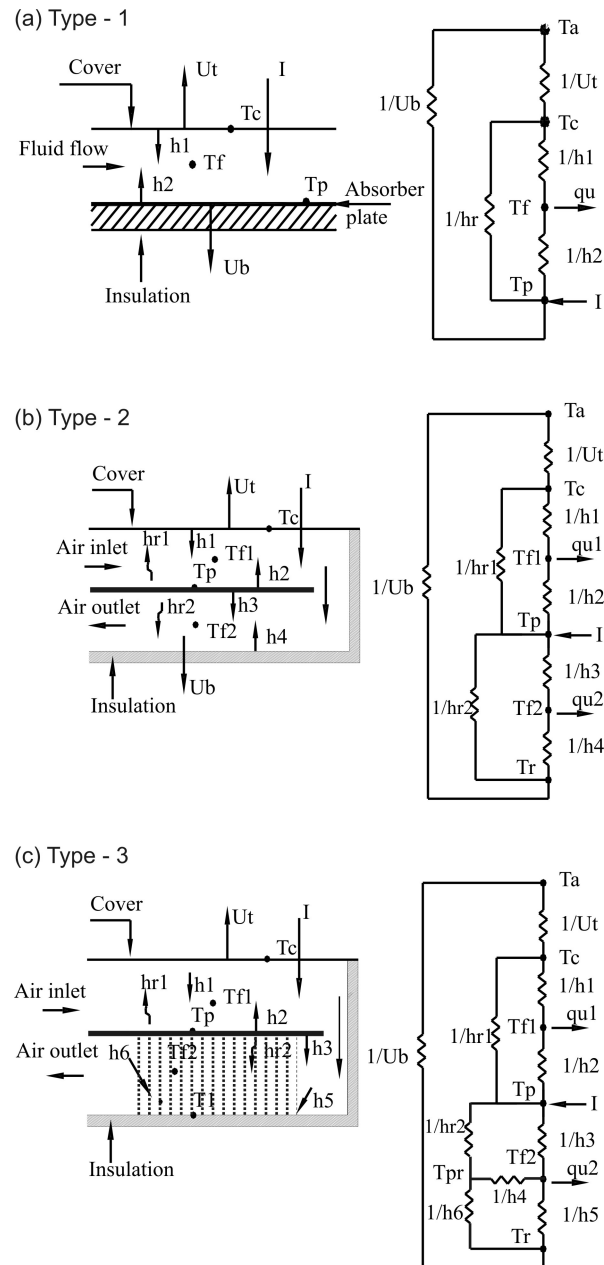


Fig. 1. Schematic diagram of the solar air heaters with thermal network: (a) Type-1, (b) Type-2, (c) Type-3.

*a) Type-1*

Collector cover:

$$h_1(T_f - T_c) + h_r(T_p - T_c) = U_t(T_c - T_a), \quad (1)$$

flat plate absorber:

$$U_b(T_p - T_a) + h_2(T_p - T_f) + h_r(T_p - T_c) = I\tau\alpha, \quad (2)$$

fluid medium:

$$h_1(T_c - T_f) + h_2(T_p - T_f) = \left(\frac{\dot{m}C_p}{W}\right) \left(\frac{dT_f}{dx}\right). \quad (3)$$

*b) Type-2*

Collector cover:

$$h_1(T_{f1} - T_c) + h_{r1}(T_p - T_c) = U_t(T_c - T_a), \quad (4)$$

fluid 1:

$$h_2(T_p - T_{f1}) = \left(\frac{\dot{m}C_{p1}}{W}\right) \left(\frac{dT_{f1}}{dx}\right) + h_1(T_{f1} - T_c), \quad (5)$$

absorber:

$$I\tau\alpha = h_{r1}(T_p - T_c) + h_2(T_p - T_{f1}) + h_3(T_p - T_{f2}) + h_{r2}(T_p - T_r), \quad (6)$$

fluid 2:

$$h_3(T_p - T_{f2}) = \left(\frac{\dot{m}C_{p2}}{W}\right) \left(\frac{dT_{f2}}{dx}\right) + h_4(T_{f2} - T_r), \quad (7)$$

bottom plate:

$$h_4(T_{f2} - T_r) + h_{r2}(T_p - T_r) = U_b(T_r - T_a). \quad (8)$$

*c) Type-3*

Collector cover:

$$h_1(T_{f1} - T_c) + h_{r1}(T_p - T_c) = U_t(T_c - T_a), \quad (9)$$

fluid 1:

$$h_2(T_p - T_{f1}) = \left( \frac{\dot{m}C_{p1}}{W} \right) \left( \frac{dT_{f1}}{dx} \right) + h_1(T_{f1} - T_c), \quad (10)$$

absorber:

$$I\tau\alpha = h_{r1}(T_p - T_c) + h_2(T_p - T_{f1}) + h_3(T_p - T_{f2}) + h_{r2}(T_p - T_{pr}), \quad (11)$$

fluid 2:

$$h_3(T_p - T_{f2}) = \left( \frac{\dot{m}C_{p2}}{W} \right) \left( \frac{dT_{f2}}{dx} \right) + h_4(T_{pr} - T_{f2}) + h_5(T_{f2} - T_r), \quad (12)$$

porous media:

$$h_{r2}(T_p - T_{pr}) + h_6(T_{pr} - T_r) = h_4(T_{pr} - T_{f2}), \quad (13)$$

bottom plate:

$$h_5(T_{f2} - T_r) + h_6(T_{pr} - T_r) = U_b(T_r - T_a). \quad (14)$$

The thermal efficiency, which is defined as the ratio of the useful energy to the total incident solar radiation, is expressed by the Hottel-Whillier-Bliss equation [8]:

$$\eta = \frac{Q_u}{AI} = F_R(\tau\alpha) - F_R U \frac{(T_i - T_a)}{I}. \quad (15)$$

## 2.1. Heat transfer coefficients

The convective heat transfer coefficient to the ambient air [9]:

$$h_{c,ga} = 5.7 + 3.8V. \quad (16)$$

The radiation heat transfer coefficient from the absorber to the glass cover can be stated as by Ratna et al. and Duffie and Beckman [2, 8]:

$$h_r = \frac{\sigma(\bar{T}_p^2 + \bar{T}_c^2)(T_p + T_c)}{\frac{1}{\varepsilon_p} + \frac{1}{\varepsilon_c} - 1}. \quad (17)$$

In addition, the radiation heat transfer coefficient from the absorber to the base plate can be written as follows:

$$h_{r2} = \frac{\sigma(\bar{T}_p^2 + T_r^2)(T_p + T_r)}{\frac{1}{\varepsilon_p} + \frac{1}{\varepsilon_r} - 1}. \quad (18)$$

The convective heat transfer coefficients are calculated using the following relations:

$$h = \frac{Nuk}{D_h}, \quad (19)$$

$$Nu = 0.0158(Re)^{0.8}, \quad (20)$$

$$Re = \frac{\dot{m}D_h}{A_f\mu}, \quad (21)$$

$$D_h = 4 \frac{\text{cross sectional area of the flow}}{\text{wetted perimeter}}. \quad (22)$$

## 2.2. Pressure drop

When the air flows through the channel in the air heater, due to friction the air pressure drops along the length of the flow channel. This pressure drop across the flow duct is given by the following expression [2]:

$$p = f \left( \frac{m^2}{\rho} \right) \left( \frac{L}{D} \right)^3, \quad (23)$$

$$f = f_0 + y \left( \frac{D}{L} \right). \quad (24)$$

The values of  $f_0$  and  $y$  are:

$$f_0 = 24/Re, \quad y = 0.9 \quad \text{for laminar flow } (Re < 2550),$$

$$f_0 = 0.0094, \quad y = 2.92Re^{-0.15} \quad \text{for transitional flow } (2550 < Re < 10^4),$$

$$f_0 = 0.059Re^{-0.2}, \quad y = 0.73 \quad \text{for turbulent flow } (10^4 < Re < 10^5).$$

### 3. Simulation procedure

A prototype internet-based computer program was developed to support the design of solar air heaters used for drying agricultural products in Malaysia. Dreamweaver<sup>TM</sup> combined with the Active Server Pages (ASP) as an extension environment, have been chosen as a development software tool. The programmatic code was written by VBScript as scripting language to execute commands on a computer [6]. Rules have been used to specify a set of action performed for a given situation. The required data are classified into three groups, the general input data concerning about meteorological conditions, the collector characteristics data that contain all specific manufacturing attributes related to the collector and the energy characteristics data which contain measured data about inlet temperature and mass flow rate related to the transfer media inside the collector [7].

Numerical values of different parameters such as outlet temperature, efficiency and the pressure drop were computed corresponding to an ambient temperature 33 °C, solar radiation 500 W m<sup>-2</sup>, air velocity 1.5 m sec<sup>-1</sup>, inlet temperature of 35 °C and different values of mass flow rate. The detailed specifications of the data for all types of solar air heaters considered in this study are given in Table 1.

Table 1. Specification for solar air heaters

Collector tilt angle [degree]	10
Collector length [m]	2.4 and 1.5
Collector width [m]	1.2
Depth [m]	0.01, 0.015, 0.02 and 0.035 for Type-1
Upper depth [m]	0.035 for Type-2 and Type-3
Lower depth [m]	0.03, 0.045, 0.06 and 0.075 for Type-2 and Type-3
Plate type	flat plate
Absorber material	black steel, $\alpha = 0.9$ and $\varepsilon = 0.85$
Cover material	ordinary clear glass, $\tau = 0.85$
Number of cover	1
Insulation material	fibre glass, $k = 0.045 \text{ W m}^{-1} \text{ K}^{-1}$
Back insulation thickness [m]	0.05
Edge insulation thickness [m]	0.05
Porous media	glass-wool of 0.8 porosity for Type-3

### 4. Results and discussion

#### 4.1. Single pass flat plate collector (Type-1)

The computed values of the efficiency, outlet temperature and pressure drop for the single pass flat plate collector plotted against different values of mass flow rate for two flow channel lengths are given in Figs. 2-4.



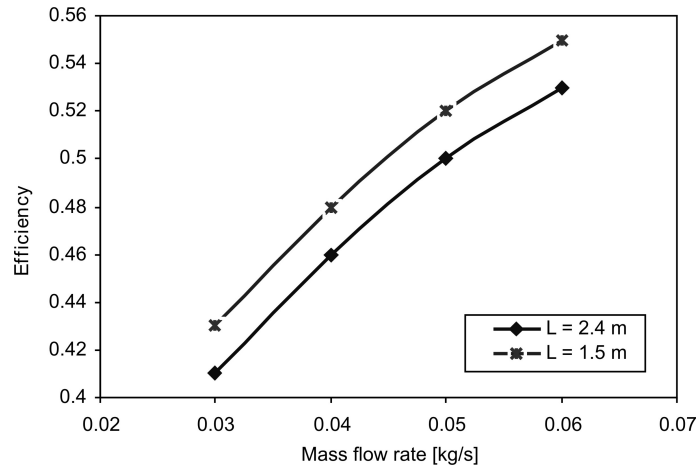


Fig. 2. Variation of efficiency with mass flow rate (Type-1).

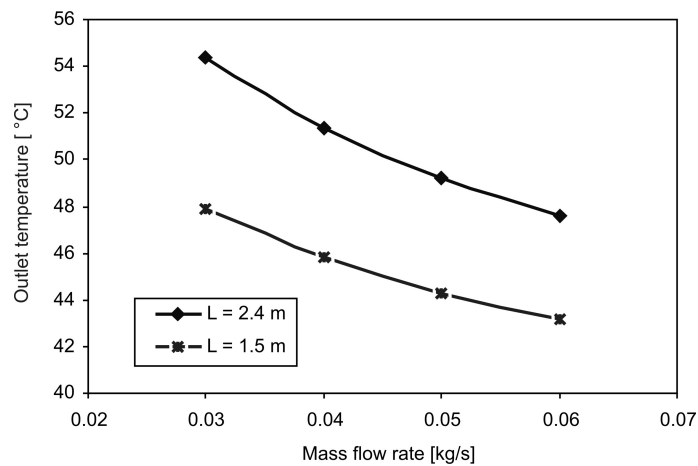


Fig. 3. Variation of outlet temperature with mass flow rate (Type-1).

It is shown that the efficiency increased with increasing mass flow rate, while the outlet temperature decreased with increasing mass flow rate. In addition, the efficiency decreased with increasing the collector length from 1.5 m to 2.4 m (Figs. 2 and 3). Figure 4 illustrates the variation of the pressure drop with the mass flow rate for collector flow length of 1.5 m and 2.4 m. It is shown that the pressure drop is a function of mass flow rate and the collector length. Pressure drop increases with increasing mass flow rate and collector length.

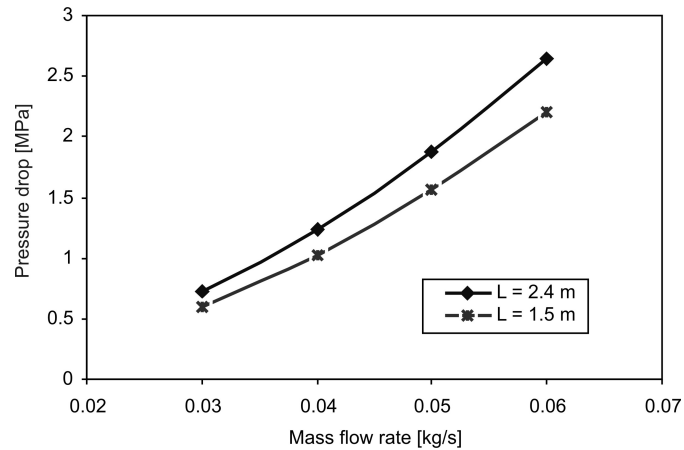


Fig. 4. Variation of pressure drop with mass flow rate (Type-1).

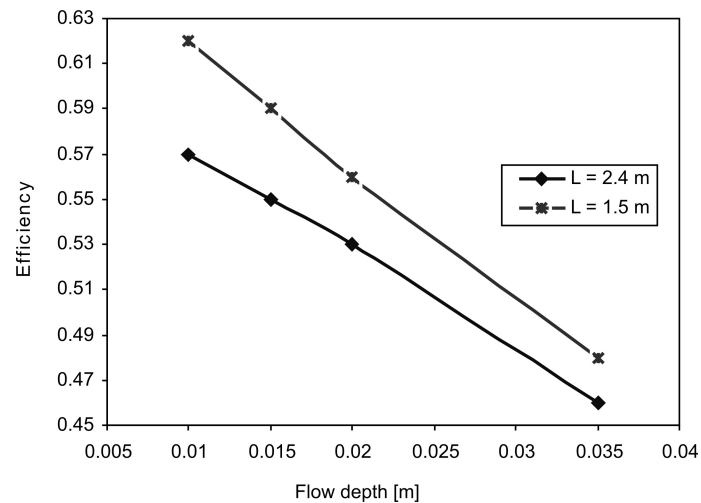


Fig. 5. Variation of efficiency with channel flow depth (Type-1).

The variation in efficiency and pressure drop with flow channel depth for different collector lengths 2.4 m and 1.5 m are displayed in Figs. 5 and 6 respectively at fixed mass flow rate of  $0.04 \text{ kg sec}^{-1}$ . Figure 5 indicates that at fixed mass flow rate the efficiency is decreased with the increase of flow channel depth, and this effect is more predominant for longer flow channel. Figure 6 illustrates that the pressure drop increases with the decrease in the flow depth, and this increase is higher for longer channel flow. The variation in outlet temperature with the flow

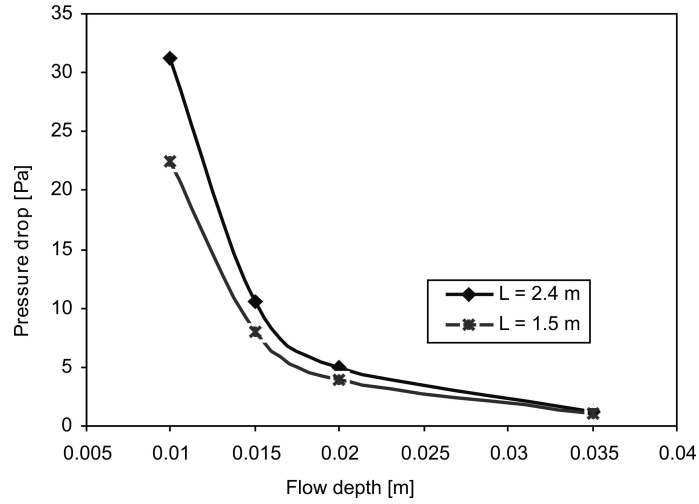


Fig. 6. Variation of pressure drop with channel flow depth (Type-1).

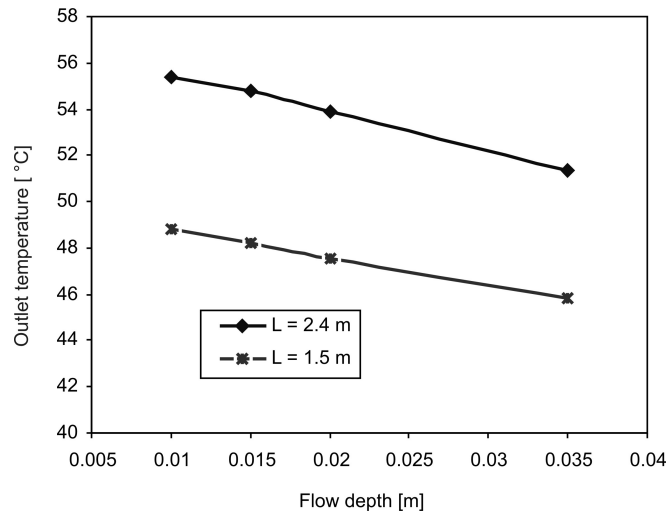


Fig. 7. Variation of outlet temperature with channel flow depth.

channel depth is displayed in Fig. 7, which indicates that the outlet temperature can be increased with decreasing flow depth.

#### 4.2. Double pass flat plate collector with and without porous media (Type-2 and Type-3)

The variation of efficiency, outlet temperature and pressure drop with different mass flow for Type-2 and Type-3 are shown in Figs. 8-10. With the increase in the mass flow rate the thermal efficiency of the system increases and this increment is more pronounced for short channel length. On the other hand the outlet temperature is decreased with the increase of mass flow rate, but this decrease is less for long channel length. By comparing the values of the efficiency and outlet temperature for Type-2 and Type-3, it is found that the use of porous media in Type-3 increases the system efficiency by 5-8% and the outlet temperature from 3-7°C. This increase causes an increase in the pressure drop for Type-3, which means

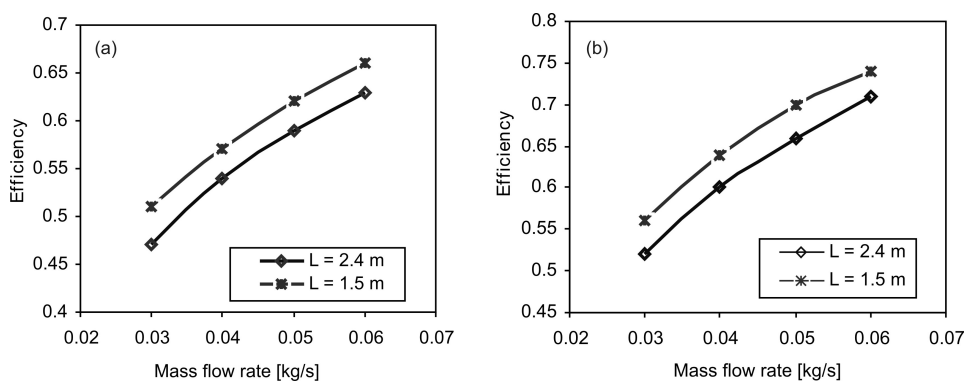


Fig. 8. Variation of efficiency with mass flow rate: (a) Type-2, (b) Type-3.

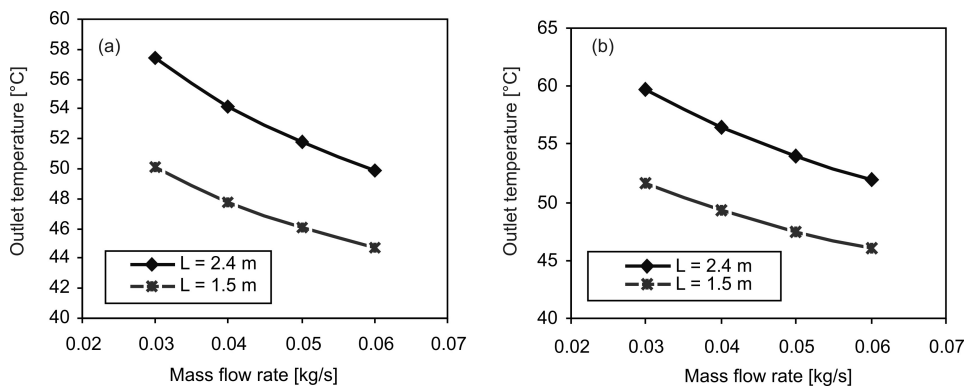


Fig. 9. Variation of outlet temperature with mass flow rate: (a) Type-2, (b) Type-3.

increasing the cost of the pumping power expended in the collector as shown in Fig. 10.

The effect of lower channel depth on the pressure drop, efficiency and outlet temperature for Type-2 and Type-3 is conducted and displayed on Figs. 11–13 for fixed mass flow rate of  $0.04 \text{ kg sec}^{-1}$  and two different flow channel lengths of 2.4 m and 1.5 m. The graphs illustrate that, with the increase of lower channel depth, the pressure drop decreased as well as the efficiency and the outlet temperature decreased.

The short channel length 1.5 m has an effect on the pressure drop and system efficiency, since it increases the system efficiency and at the same time it decreases the pressure drop. But the outlet temperature is higher for long channel length 2.4 m than for the short one 1.5 m.

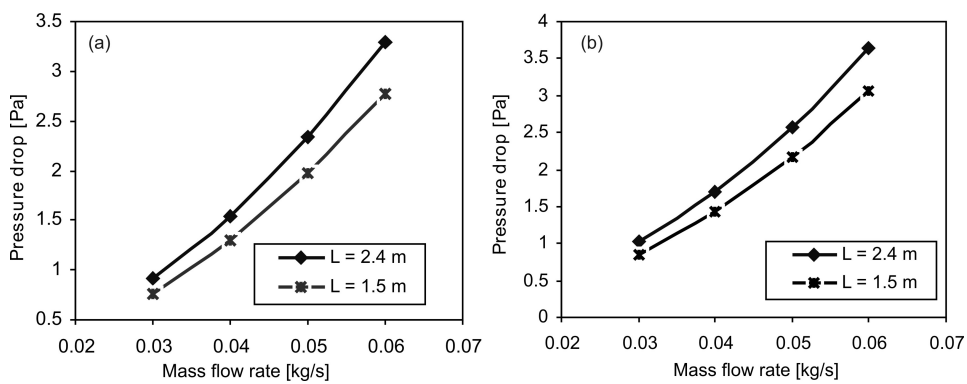


Fig. 10. Variation of pressure drop with mass flow rate: (a) Type-2, (b) Type-3.

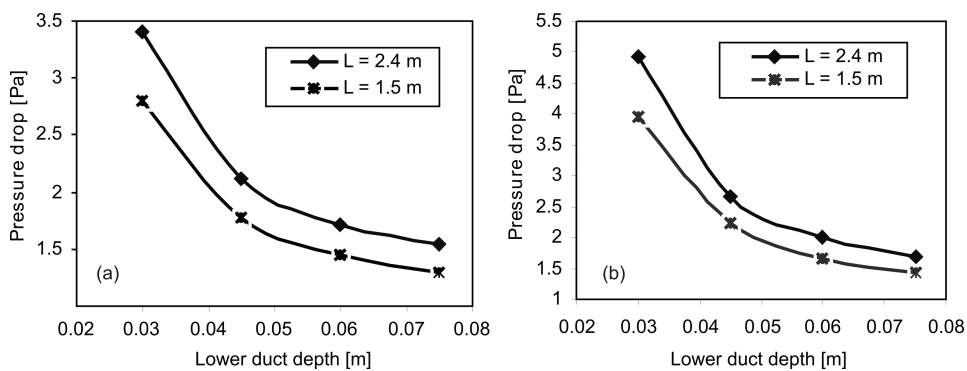


Fig. 11. Variation of pressure drop with lower channel depth: (a) Type-2, (b) Type-3.

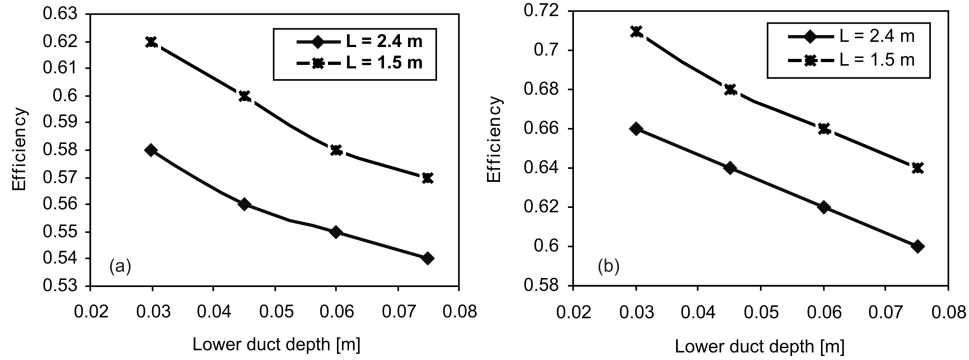


Fig. 12. Variation of efficiency drop with lower channel depth: (a) Type-2, (b) Type-3.

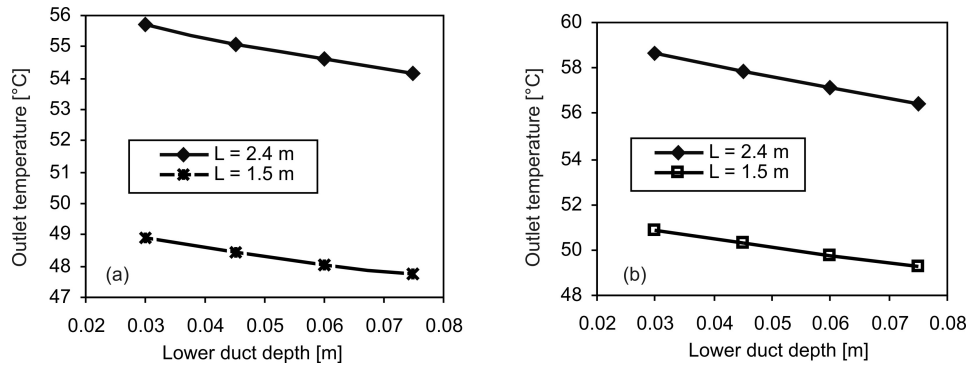


Fig. 13. Variation of outlet temperature with lower channel depth: (a) Type-2, (b) Type-3.

An analysis of the values in different figures for Type-1, Type-2 and Type-3 at the same configuration and parameters: mass flow rate  $0.04 \text{ kg sec}^{-1}$ , channel length 2.4 m, flow depth 0.035 m and 0.045 m lower channel depth in double flow (Type-2 and Type-3) was carried out. It is found that the system thermal efficiency increases by 10–12% in double flow mode Type-2 when compared to the single flow Type-1 and increases by 8% after using porous media in the lower channel Type-3 when compared to the double flow without porous media Type-2. Therefore the system efficiency increases by 18% after using porous media in the lower channel Type-3 when compared to the single flow pass Type-1. At the same time the pressure drop will be increased, thus increasing the pumping power expanding by about 3–4 times.

## 5. Validation

Validation and verification focus on the comparison between the predicted output and the experimental results for each solar air heater type. The experimental results have been published by Karim and Hawlader [5] for flat plate collector in single and double pass mode, while El-Radi [10] has done an experiment on the double pass flat plate collector with porous media in the lower duct.

An output from the mathematical simulation has been run according to the same configuration and parameters done in experimental work by Karim and Hawlader [5] and Elradi [10]. A great agreement has been occurred between the experimental results and the predicted output when comparison has been achieved with an error deficiency equal to 5 % at maximum.

## 6. Conclusion

A mathematical simulation to predict the effect of different parameters on system thermal performance and pressure drop, for flat plate collector in single and double flow mode with and without using a porous media, has been conducted. It is found that increasing the mass flow rate through the air heaters results in higher efficiency but also the pressure drop is increased. On the other hand decreasing the channel flow depth results in increasing the system efficiency and outlet temperature at the same time the pressure drop increased.

The channel length also has an effect on the thermal efficiency hence the system efficiency is more increased for the short channel length than for the long one, while the pressure drop is less than the pressure drop in long channel length.

The double flow is more efficient than the single flow and the use of porous media increases the system efficiency and the outlet temperature. This increment will result in the increase of the pressure drop thus increasing the pumping power expanded in the collector.

Finally the adoption of the aforementioned internet based mathematical simulation that has been developed to predict the thermal performance of solar air heaters, and to find the influence of different parameters seems to be promising, hence it is capable to predict reasonable results according to chosen parameters with design rules that incorporate the human expertise in the field. What is more, the use of internet will help in sharing and distributing the knowledge.

This process should be of interest to designers and engineers who like to compare the cost effectiveness of solar air heaters.

In the near future the computer program shall encompass the V-groove absorber in single and double pass and the economic aspect for the different types of solar air heaters.

## REFERENCES

- [1] MOHD, Y. H.—BAHARUDIN, Y.—DAUD, W. R. W.: Kementerian Sams, Teknologi dam Alam Sekitar, 1, 1999, p. 206.
- [2] RATNA VERMA—RAM CHANDRA—GARG, H. P.: Renewable Energy, 1, 1991, p. 361.
- [3] RATNA VERMA—RAM CHANDRA—GARG, H. P.: Renewable Energy, 2, 1992, p. 521.
- [4] CHOUDHURY, C.—CHAUHAN, P. M.—GARG, H. P.: Heat Recovery System & CHP, 15, 1995, p. 755.
- [5] KARIM, M. A.—HAWLADER, M. N. A.: Energy Conversion and Management, 45, 2004, p. 329.
- [6] BASHRIA, A. A.—ADAM, N. M.—SAPUAN, S. M.—DAUD, M.—OMAR, H.—AHMED, M. H. M.—ABAS, F.: Part A: Journal of Power and Energy, Proceedings of the Institution of Mechanical Engineers, 218, 2004a, p. 579.
- [7] BASHRIA, A. A.—ADAM, N. M.—DAUD, M.—OMAR, H.—AHMED, M. H. M.—ELRADI, A. MUSA: Journal of Energy & Environment, 3, 2004b, p. 91.
- [8] DUFFIE, J. A.—BECKMAN, W. A.: Solar Engineering of Thermal Processes. Toronto, John Wiley&Sons, Inc. 1991.
- [9] McADAMS, W. H.: Heat Transmission. 3<sup>rd</sup> ed. New York, McGraw-Hill 1954.
- [10] EL-RADI, A. M.: Thermal performance of the double pass solar air collector with and without porous media. [M.Sc. Thesis]. Bangi, Malaysia, Faculty of Engineering, Universiti Kebangsaan 2001.

*Received: 24.10.2007*

*Revised: 30.12.2008*